Oscillations in hydrothermal systems as a source of periodic unrest at caldera volcanoes: Multiparameter insights from Nisyros, Greece

Journal Item

Oscillations in hydrothermal systems as a source of periodic unrest at caldera volcanoes: Multiparameter insights from Nisyros, Greece

Joachim Gottsmann[1]*, Roberto Carniel[2], Nicolas Coppo[3], Luke Wooller[4], Stefanie Hautmann[1], Hazel Rymer[4]

[1]Department of Earth Sciences, University of Bristol, Wills Memorial Building, Queen's Road, Bristol, BS8 1RJ, United Kingdom

[2]Dipartimento di Georisorse e Territorio, Università di Udine, Via Cotonificio 114, 33100 Udine, Italy

[3]Institute of Geology and Hydrogeology, University of Neuchâtel, 11 Rue Emile Argand / CP 158, 2009 Neuchâtel, Switzerland

[4]Department of Earth Sciences, The Open University, Milton Keynes, MK7 6AA, United Kingdom

*Corresponding author (e-mail: j.gottsmann@bristol.ac.uk).

Abstract

Unrest at collapse calderas is generally thought to be triggered by the arrival of new magma at shallow depth. But few unrest periods at calderas over the past decades have culminated in volcanic eruptions and the role of hydrothermal processes during unrest is drawing more and more attention. Here we report joint and simultaneous continuous multi-parameter observations made at the restless Nisyros caldera (Greece), which reveal non-steady short-term oscillatory signals. The combined geodetic, gravimetric, seismic and electromagnetic records indicate that the oscillations are associated with thermohydromechanical disturbances of the hydrothermal system. The dominant period of oscillation (40-60 min) indicates short-term processes most likely associated with instabilities in the degassing process. Amplitudes of recorded geodetic and gravimetric signals are comparable to amplitudes observed at other periodically restless calderas. We conclude that shallow aqueous fluid migration can contribute significantly to periodic unrest, explaining the lack of eruptions in many cases of unrest.

Introduction

Several studies have concluded that magma emplacement at depth is the dominant source of caldera unrest [*Newhall and Dzurisin*, 1988; *Dzurisin*, 2003; *Wicks, et al.*, 2006] causing quantifiable geophysical signals at the surface for weeks, months or even years. But few unrest periods at calderas over the past few decades have culminated in a volcanic eruption and it may be that aqueous fluid migration at depth results in similar signals [*Bonafede and Mazzanti*, 1998, *Battaglia, et al.*, 2006]. Clearly, the dilemma is how to discriminate signals from magma movement from signals originating from fluid flow and thus to assess the likelihood of an impending eruption. Observations of ground deformation are regarded as a standard tool for monitoring reservoir replenishment at depth [*Dzurisin*, 2003; *Poland, et al.*, 2006; *Dvorak and Dzurisin*, 1997]. Unfortunately, geodetic observations alone cannot resolve the cause of ground movements [*Wicks, et al.*, 1998], but in combination with gravimetric observations the data can shed light on source characteristics [*Battaglia, et al.*, 2003; *Gottsmann, et al.*, 2006]. An inherent problem is that periodic measurements may suffer from data aliasing, that is, the obtained times series give a distorted representation of the frequency of mass changes at depth [*Rymer*, 1994]. In many cases, this frequency coincides with the frequency corresponding to the survey interval and thus the real period of signals triggered by dynamic changes in the sub-surface remains ambiguous. Clear evidence for a hydrothermal contribution to geophysical signals recorded during time-lapse observations had been found only in a very limited number of cases [*Todesco*, 2005, *Tikku, et al.*, 2006], and information on the frequency of the kinematics from multiparametric investigations is rare. In this paper we present an integrated multi-parameter geophysical data set collected at the Nisyros caldera in Greece. These data reveal fundamental short-term processes most likely related to instabilities in the degassing process within hydrothermal aquifers. Thermohydromechanical (THM) disturbances are caused by the release and upward migration of hydrothermal fluids inducing oscillatory geophysical signals.

Background

The study area is the central caldera of Nisyros Island (Greece; Fig. 1a), which underwent 14 cm of ground uplift during a volcano-seismic crisis in the mid-1990s [*Lagios, et al.*, 2005]. The caldera is believed to have formed during a large-scale eruption about 25ka before present and was subsequently partly refilled by dacitic domes [*Limburg and Varekamp*, 1991]. Historic eruptions are limited to phreatic explosions as evidenced by numerous craters in the south-eastern part of the caldera. Along the caldera floor and the southern caldera wall, surface expressions of an active hydrothermal system include hydrothermal deposits, fumaroles, mud pools and boiling water pools [*Caliro, et al.*, 2005; *Chiodini, et al.*, 2002]. The current model [*Caliro, et al.,* 2005] of the subsurface structure beneath the caldera features i) a magmatic body, at unknown depth, which supplies heat and fluids to the hydrothermal system, (ii) a deep boiling aquifer (situated at more than 900 m below sea level), and (iii) shallow reservoir(s) at variable temperatures fed by a mixture of vapor separated by the deep aquifer and meteoric water.

Gottsmann, et al., [2005] showed that the amplitude of residual gravity changes (corrected for the effect of ground deformation on gravity) observed within the caldera between two measurement campaigns (November 2003 and October 2004) were also detected over time scales of tens of minutes, indicating the presence of fundamental short-term dynamic changes in the sub-surface. Benchmarks located well outside the caldera (on the flanks of the central edifice) did not show such short-term variations. The short-term residual gravity changes found inside the caldera were on the same order of magnitude as gravity variations recorded during traditional time-lapse surveys, for example at the Campi Flegrei caldera [*Berrino*, 1994; *Gottsmann, et al.*, 2003].

Results from new field experiment and interpretation

In order to obtain a more detailed insight into the short-term subsurface dynamics at the caldera, we devised a 10-day multi-parameter geophysical experiment in May 2006 including the following instrumentation and observation frequencies: (i) one automated continuously recording (1 Hz) gravimeter (Lacoste&Romberg model D-41), (ii) two gravimeters (Lacoste&Romberg model G-403 and G-513) manually read at 0.003 Hz for a total of about 30 hours, (iii) 4 Leica GPS 500 receivers (1 Hz), (iv) one Lennartz LE-3D/5s seismometer (125 Hz), (v) one very low frequency (VLF; 15-250 kHz; sampling frequency of 4 Hz) electromagnetic receiver. The instrumentation was deployed jointly in areas previously identified as being affected by short-term changes [*Gottsmann, et al.*, 2005] and more than 120 h of simultaneous records were collected. For clarity, we have low-pass (1 min) filtered all records. In this paper, we focus on 2 data sets: a 24 hr record on May 16, 2006 and a 4 hr record on May 19, 2006. These were selected for the following reasons: (i) on May 16, ground deformation, gravity changes and seismicity were recorded at the same location while the VLF record was obtained ca. 600 m to the south-west, inside a phreatic crater hosting boiling mudpools and fumaroles, enabling a spatial separation of the origins of signals observed by the different instruments (Fig. 1b), (ii) we recorded two teleseismic events that day which allow us to assess the caldera system's response to external triggers

(Fig. 1b), (iii) we can employ the data set to monitor an instability in the subsurface dynamics which we interpret to be a key phenomena for the understanding of processes at restless calderas with hydrothermal activity (Fig. 2), and (iv) using both May 16 and 19 records, the data enable a direct quantification of the timescale of short-term cyclic oscillations at the caldera (Fig. 3).

Figures 1b-c present joint records (continuous gravity, GPS, VLF, seismicity) of May 16, 2006, including signals caused by 2 teleseimic events. Note, that all gravimetric data shown is corrected for the effect of Earth and Ocean tides. Focusing on the record preceding the teleseismic events, the continuous gravimetric signal shows a roughly periodic oscillation with maximum amplitudes of 0.015 mGal (Fig. 1c). The GPS data correlates with the gravimetric record (e.g., min 100-250), whereby ground subsidence is matched by gravity decrease. This is the opposite behaviour one would expect if the gravimeter is responding solely to ground deformation (a free air effect results in a gravity increase with ground subsidence). Interestingly though, the GPS record displays several spikes (at t = 30 min, 300 min, 450 min and 520 min) indicating relative ground motion of up to 0.15 m whereas the GPS RMS (root mean square error) rarely exceeds 0.04 m. Particularly, the min 445 event is associated with a RMS of less than 0.02 m. We can exclude poor satellite coverage or multipath as sources for the observed ground deformation as well as sidereal effects. Similar short-term ground deformation was recently also observed at the Yellowstone caldera [*Tikku, et al.*, 2003].

The gravity record associated with this event shows a small local maximum, yet the seismic record indicates a clear spike in the intensity data. Gravimetric data reduction for the effect of ground deformation assuming a Bouguer density of 2100 kg/m3 for caldera fill rocks, results in a residual gravity waveform with average amplitudes of 0.02 mGal (Fig.

2a). The 450 min event, however, translates into a maximum gravity amplitude of 0.030 mGal. So far, all instrumentation deployed at the same location responded to the min 450 event, but what can be learned from the VLF data recorded inside the phreatic crater? Figure 2b shows the 20.8 kHz In Phase record together with seismic intensity. We observe a clear break in slope in the VLF record, coinciding with the seismic intensity peak around 450 min. But it is not for another 18 min, before the VLF signal peak indicates a clear change in the electric structure of the ground. Given the low electrical resistivity of the ground, the depth penetration of the 20.8 kHz electromagnetic signal is estimated to be about 35 m. We thus infer the event detected in the GPS, gravimetric and seismic record translates into a change of the secondary induced electromagnetic field below the crater floor. A similar response is also observable at 490 min, again coinciding with a peak in seismic intensity. Unfortunately, no GPS data is available for this event, but the observed gravity data shows a small local minimum. After 500 min, the VLF data indicates stable electromagnetic properties of the shallow subsurface, that seem to be unaffected by subsequent peaks in seismic intensity (whose waveforms seem to indicate an anthropogenic origin).

The seismic waveforms of the 450 (Fig. 2b), 480 and 490 min events suggest tremor episodes rather than discrete events with a sharp onset and look similar to seismic records from the caldera [*Caliro, et al.*, 2005], which were interpreted to reflect instabilities in the degassing process at shallow depth (400-800 m below caldera floor). However, since our seismic setup does not allow us to constrain their depth, we cannot exclude the deep hydrothermal aquifer inferred to be located between 1300 and 1800 m below the caldera floor as the source region for these seismic signals. Caliro and coworkers [*Caliro, et al.*, 2005] found evidence for the interaction of hydrothermal/magmatic fluids with their host rocks at that depth from long-period (LP) seismic events. We have so far not detected discrete single LP events in the record of May 16, but low frequency energy (below 2 Hz) is present in the continuous seismic record. Similar tremor waveforms were observed during degassing activity at open conduit volcanoes such as Stromboli [*Ripepe, et al.*, 2002], Erta Ale [*Jones, et al.*, 2006] and Ambrym [*Carniel, et al.*, 2003], and interpreted as the superposition of a series of discrete bursts, an interpretation that we also propose here. We thus associate aforementioned bursts with instabilities during magmatic degassing, but cannot provide unambiguous information on their source location. In another study, using a multiday gravimetric record, Tikku et al. (2006) interpret variations in microseimicity recorded in an active geyser basin at the Yellowstone caldera (USA) as tremor induced by fluid flow.

We present the following model to explain the observed signals:

i) The tremor result from a sudden THM disturbance of the hydrothermal system triggering, or being caused by, a pressure variation. An effective cause of pressure variations is the non-steady degassing of the deep magma reservoir, feeding a deep-seated boiling aquifer at temperatures of around 340 ˚C [*Caliro et al.,* 2005 and references therein]. Supercritical fluids are a very effective source for sudden volume variations translating into abrupt pressure changes. In our model, a sudden pressure increase by, for example anomalous, degassing at depth translates into elastic surface deformation. The associated gravity increase is predominantly caused by the Bouguer effect of deformation, and the resulting propagation of density boundaries in a planar reservoir [*Walsh and Rice*, 1979, *Battaglia, et al.*, 2006].

ii) The THM disturbance causing the tremor signal is explained by the coalescence and rise of bubbles.

iii) Pressurisation dissipates by the upwards release of fluids and vapor (two-phase flow) along (newly created) fractures and faults resulting in ground subsidence and residual gravity decrease.

iv) Vapor and fluid separated from the deeper high temperature aquifer recharge the shallower, lower temperature reservoirs, where their arrival changes the electrical properties of the crater fill as seen by the VLF measurements.

We perform a rough calculation using the inferred source depth and the delay time of the electromagnetic signal to quantify average ascent speeds of the two-phase flow. Since the source depth cannot be unambiguously constrained (most likely the shallow or deep hydrothermal system), we present a possible range of speeds from 0.4 m/s to 1.4 m/s. These speeds are on the order of magnitude found for nonpropagative THM disturbances and pressure shock waves [*Revil, et al.*, 2003].

Conclusions

Our analysis presents the first quantitative study of the background dynamic processes at a restless caldera. The dominant period of oscillation (40-60 min, Fig. 2d and 3b) indicates short-term processes most likely associated with instabilities in the degassing process, whereby bubbles coalesce and rise through a complex hydrothermal system. These processes constitute the majority of geophysical signals recorded at the ground surface and hence dominate activity at this restless caldera. Given the number of phreatic craters formed in the caldera in historic times, hydrothermal explosions pose a serious hazard on the island. With several hundreds of day visitors to the hydrothermal area during the summer months, a significant number of people are at direct risk from sudden catastrophic discharges. The trigger mechanisms of such instabilities in the hydrostatic liquid column are still poorly understood, and forecasting of phreatic activity is intrinsically difficult and associated with a high degree of uncertainty. Integrated data sets such as those presented here may help identify key parameters and their dynamic range during background mode, which may enable forecasting when a system develops from background activity to a state where catastrophic discharge is to expected. Aqueous fluid migration must be regarded as an important causative mechanism for unrest and efforts should be made to obtain multi-parameter continuous time series. Magmatic signals must exceed shallow hydrothermal signals in order to be seen during geophysical monitoring programs.

Acknowledgments

Support is acknowledged from a Royal Society University Research Fellowship to JG, from the Italian PRIN project 2004131177 ‘‘Numerical and graphical methods for the analysis of time series data’’ to RC, from the Laboratory of Geomagnetism, IGH, University of Neuchâtel to NC, and the Bayerische Forschungsstiftung DPA-53/05 to SH. We thank P. Coppo, J. Scott and K. Pimm for priceless field assistance. The paper benefited from constructive comments by M. Battaglia and D. Tedesco.

References

Battaglia, M., et al. (2003), The mechanics of unrest at Long Valley caldera, California. 2. Constraining the nature of the source using geodetic and micro-gravity data, *Journal of Volcanology and Geothermal Research*, *127*, 219-245.

Battaglia, M., et al. (2006), Evidence for fluid migration as the source of deformation at Campi Flegrei caldera (Italy), *Geophysical Research Letters*, *33*, L01307, doi:01310.01029/02005GL024904.

Berrino, G. (1994), Gravity changes induced by height-mass variations at the Campi Flegrei caldera, *Journal of Volcanology and Geothermal Research*, *61*, 293-309.

Bonafede, M., and M. Mazzanti (1998), Modelling gravity variations consistent with ground deformation in the Campi Flegrei caldera (Italy), *Journal of Volcanology and Geothermal Research*, *81*, 137-157.

Caliro, S., et al. (2005), Recent activity of Nisyros volcano (Greece) inferred from structural, geochemical and seismological data, *Bulletin of Volcanology*, *67*, 358-369.

Carniel, R., et al. (2003), Spectral and dynamical transitions on the hours-to-days timescale, Ambrym, Vanuatu (July-August 2000), *Journal of Volcanology and Geothermal Research*, *128*, 1-13.

Chiodini, G., et al. (2002), Geochemical evidences of an ongoing volcanic unrest at Nisyros Island (Greece), *Geophysical Research Letters*, *29*, doi10.1029/2001GL014355.

Dvorak, J. J., and D. Dzurisin (1997), Volcano Geodesy: the search for magma reservoirs and the formation of eruptive vents, *Reviews in Geophysics*, *35*, 343-384.

Dzurisin, D. (2003), A comprehensive approach to monitoring volcano deformation as a window on the eruption cycle, *Reviews in Geophysics*, *41*, doi: 10.1029/2003RG000134.

Gottsmann, J., et al. (2003), Hazard assessment during caldera unrest at the Campi Flegrei, Italy: a contribution from gravity-height gradients, *Earth and Planetary Science Letters*, *211*, 295-309.

Gottsmann, J., et al. (2006), Unrest at Campi Flegrei: A contribution to the magmatic versus hydrothermal debate from inverse and finite element modeling, *Journal of Geophysical Research*, *111*, doi:10.1029/2005JB003745.

Gottsmann, J., et al. (2005), On the interpretation of gravity variations in the presence of active hydrothermal systems: Insights from the Nisyros Caldera, Greece, *Geophysical Research Letters*, *32*, doi:10.1029/2005GL024061.

Jones, J., et al. (2006), Seismic characteristics of variable convection at Erta Ale lava lake, Ethiopia, *Journal of Volcanology and Geothermal Research*, *153*, 64-79.

Lagios, E., et al. (2005), Ground deformation of Nisyros Volcano (Greece) for the period 1995-2002: Results from DInSAR and DGPS observations, *Bulletin of Volcanology*, *68*, 201-214.

Limburg, E. M., and J. C. Varekamp (1991), Young pumice deposits on Nisyros, Greece, *Bulletin of Volcanology*, *54*, 68-77.

Newhall, C. G., and D. Dzurisin (1988), *Historical unrest at large calderas of the world*, 1108 pp., U. S. Geological Survey, Reston, VA, United States.

Poland, M., et al. (2006), The changing shapes of active volcanoes: History, evolution, and future challenges for volcano geodesy, *Journal of Volcanology and Geothermal Research, 150*, 1-13.

Revil, A., et al. (2003), The volcano-electric effect, *Journal of Geophysical Research*, *108*, DOI 10.1029/2002JB001835.

Ripepe, M., et al. (2002), Thermal, seismic and infrasonic evidences of variable degassing rates at Stromboli volcano, *Journal of Volcanology and Geothermal Research*, *118* 285-297.

Rymer, H. (1994), Microgravity change as a precursor to volcanic activity, *Journal of Volcanology and Geothermal Research*, *61*, 311-328.

Tikku, A. A., et al. (2006), Temporal fluctuations of microseismic noise in Yellowstone's Upper Geyser Basin from a continuous gravity observation, *Geophysical Research Letters*, *33*, doi:10.1029/2006GL026113.

Tikku, A. A., et al. (2003), 2002 and 2003 Gravity and GPS observations in Yellowstone's Upper Geyser Basin, *Eos Trans. AGU 84*, Abstract V52E-01.

Todesco, M. (2005), Modeling hydrothermal fluid circulation and gravity signals at the Phlegraean Fields caldera, *Earth and planetary science letters*, *240*, 328-338.

USGS (2006), http://earthquake.usgs.gov/,

Walsh, J. B., and J. R. Rice (1979), Local changes in gravity resulting from deformation, *Journal of Geophysical Research*, *84*, 156-170.

Wicks, C. J., et al. (1998), Migration of Fluids Beneath Yellowstone Caldera Inferred from Satellite Radar Interferometry, *Science*, *282*, 458 - 462.

Wicks, C. W., et al. (2006), Uplift, thermal unrest and magma intrusion at Yellowstone caldera, *Nature*, *440*, 72-75.

FIGURE CAPTIONS

Figure 1: a. Colour-coded digital elevation model (in m) of Nisyros Island, Greece, located at 36.57°N and 27.18°E in the Aegean Sea. Cross and triangle indicate approximate locations of instrumentation on May 16 and 19, 2006, respectively. b-c. Joint records (continuous gravity, GPS, VLF, seismicity) of May 16, 2006, including b. signals caused by the arrival of surface waves at min 659 from a M_w=7.4 seismic event (10:39 UTC) at the Kermadec Islands [*USGS*, 2006] and a M_w=6.8 earthquake in the Nias region of Indonesia about 5 hours later [*USGS*, 2006] (time of teleseismic events are marked by red stars). The energy of the first event dissipates quicker in the seismic record than in the gravimetric record due to the excitation of the gravimeter by the Earth's eigenmodes. The VLF In Phase (20.8 kHz) record displays a break in slope about 15-20 min later indicating a change in the electrical properties of the subsurface. c. Periodic oscillations in observed gravity and GPS data over approximately 10 h including several spikes and troughs in the GPS record, which cannot be explained by artefacts or poor satellite coverage. GPS data is reported relative to a reference located outside the caldera at. The GPS RMS (root mean square) error is below 0.03 m for these events.

Figure 2. a. Residual gravity data and RMS gravity errors and seismic intensity. Gravity data is reduced for the effect of ground deformation assuming a Bouguer density of 2100 kg/m^3 for caldera fill rocks, resulting in a periodic oscillation with average amplitudes of 0.02 mGal and a peak of 0.03 mGal, coinciding with the burst in seismic intensity at 445 min. b. The 20.8 kHz In Phase VLF and seismic intensity records. The 445 min seismic burst is matched by a break in slope in the VLF record (black broken lines) followed by a peak amplitude after a delay time of 18 min. A similar delay is seen after the 490 min event and subsequent to the M_w=7.4 teleseism a few hours later (Fig. 1b). c. Example of seismic

tremor signal recorded between 440 and 460 min ("the 450 min event"). The waveform is interpreted to represent the superposition of a series of discrete bursts in the hydrothermal system. d. Fast-Fourier-Transform (FFT) power spectrum of gravity, seismic and VLF In Phase records of the first 10 hours of May 16, 2006. The VLF and seismic time series indicate cyclic oscillatory behavior with a peak power at 43 min also seen, though to a lesser power, in the gravimetric record with a peak at 60 min. Since the gravimeter and GPS receiver were not co-located with the VLF receiver during the experiment, we attribute the differences in the periods to differences in the sub-surface dynamics at the two locations. The seismic record is more global and identifies cycles at either location. See also Figure 3.

Figure 3. Joint VLF In Phase (20.75 kHz) and observed gravity record obtained at the location marked by a triangle in Figure 1a, in a 4 m deep and 600 m long crack which opened in 2001 [*Lagios, et al.*, 2005]. This site is undergoing anomalous CO_2 degassing [*Caliro, et al.*, 2005]. The periodic oscillations of both gravity (amplitudes up to 0.02 mGal) and VLF data are inversely correlated. The FFT power spectrum is shown in the inset. The dominant period of the gravity cycles is 46 min, matching the periods of VLF and seismic data recorded at May 16 (Fig. 2d). A 46 min cycle is also visible in the VLF data, however its power peaks at 32 min/cycle. These observations are in support of our earlier speculation on the existence of significant short-term oscillations at the caldera [*Gottsmann, et al.*, 2005].

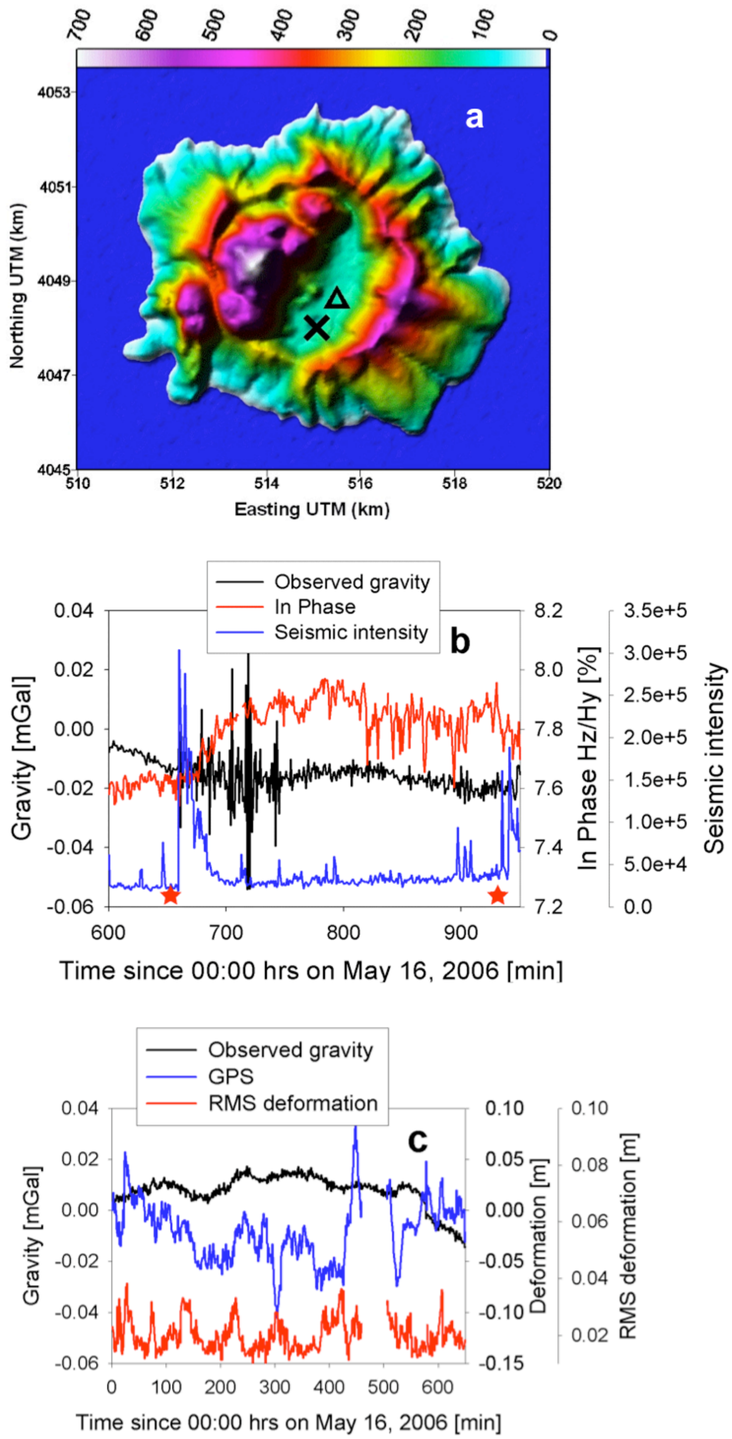
700
600
500
400
300
200
100
0
a
4053
4051
4049
4047
4045
Northing UTM (km)
510
512
514
516
518
520
Easting UTM (km)
Observed gravity
In Phase
Seismic intensity
b
Gravity [mGal]
In Phase Hz/Hy [%]
Seismic intensity
0.04
0.02
0.00
-0.02
-0.04
-0.06
8.2
8.0
7.8
7.6
7.4
7.2
3.5e+5
3.0e+5
2.5e+5
2.0e+5
1.5e+5
1.0e+5
5.0e+4
0.0
600
700
800
900
Time since 00:00 hrs on May 16, 2006 [min]
Observed gravity
GPS
RMS deformation
c
Gravity [mGal]
Deformation [m]
RMS deformation [m]
0.10
0.05
0.00
-0.05
-0.10
-0.15
0.08
0.06
0.04
0.02
0
100
200
300
400
500
600
Time since 00:00 hrs on May 16, 2006 [min]

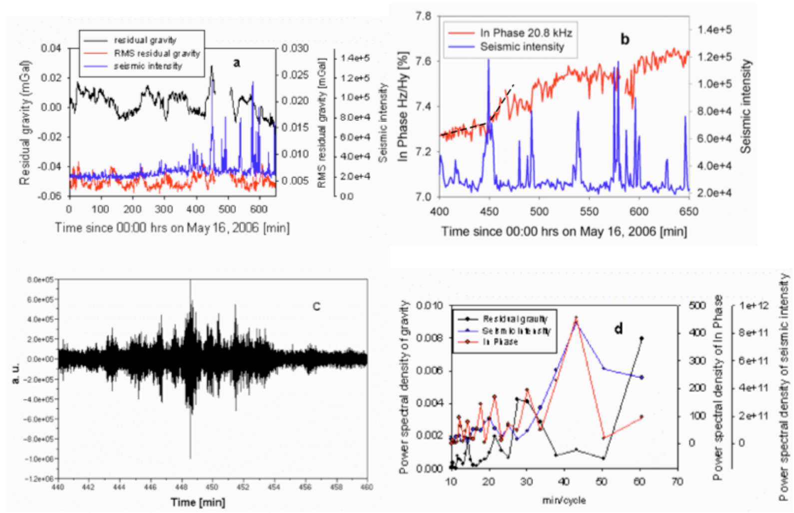
residual gravity
RMS residual gravity
seismic intensity
a
Residual gravity (mGal)
RMS residual gravity [mGal]
Seismic intensity
Time since 00:00 hrs on May 16, 2006 [min]
In Phase 20.8 kHz
Seismic intensity
b
In Phase Hz/Hy [%]
Seismic intensity
Time since 00:00 hrs on May 16, 2006 [min]
c
a. u.
Time [min]
Residual gravity
Seismic intensity
In Phase
d
Power spectral density of gravity
Power spectral density of In Phase
Power spectral density of seismic intensity
min/cycle

Figure 3

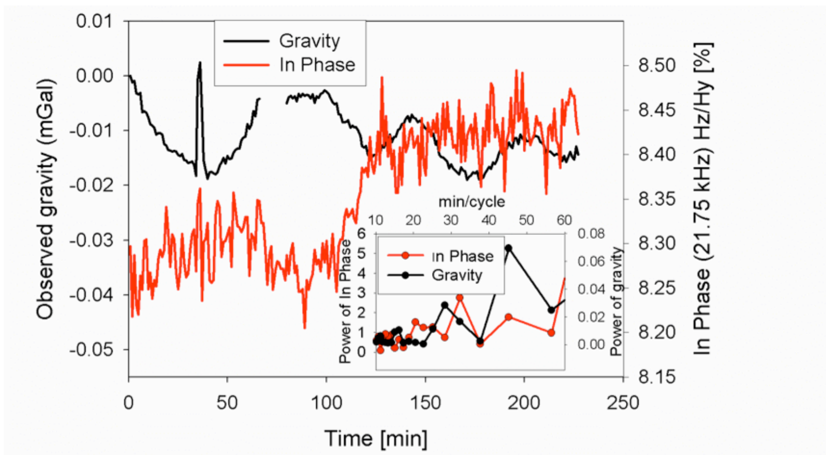

Gravity
In Phase
Observed gravity (mGal)
In Phase (21.75 kHz) Hz/Hy [%]
Time [min]
min/cycle
Power of In Phase
Power of gravity